

# Temperature dependence of the Spin-Lattice Relaxation Time of the $^{23}\text{Na}$ -NMR Line in $\text{NaNO}_2$ \*

M. Igarashi, H. Kitagawa<sup>1</sup>, S. Takahashi<sup>2</sup>, R. Yoshizaki<sup>3</sup>, and Y. Abe

Institute of Physics, University of Tsukuba, Tsukuba, Ibaraki, 305, Japan

<sup>3</sup>Institute of Applied Physics, University of Tsukuba, Tsukuba, Ibaraki, 305, Japan

Z. Naturforsch. **47a**, 313–318 (1992); received November 6, 1991

The spin-lattice relaxation time,  $T_1$ , of the  $^{23}\text{Na}$ -NMR line in  $\text{NaNO}_2$  is measured between 25 K and 160 K at two magnetic field strengths, 1.1 T and 6.9 T. The temperature dependence of  $T_1$  for the center line, observed on a polycrystalline sample prepared by precipitation from aqueous solution, is given by a monotonous curve.  $T_1$  increases gradually as the temperature decreases. On the other hand for a single crystal, which is made by a modified Bridgman method, the temperature dependence of  $T_1$  shows two deep dips below 150 K and a frequency dependence which cannot be explained by ordinary BPP theory.

The dominant relaxation mechanism above and below 150 K is also investigated.

## 1. Introduction

The spin-lattice relaxation of the magnetization of a nucleus with  $I > \frac{1}{2}$  in highly purified nonmagnetic material is usually dominated by an interaction of the nuclear quadrupole moment with thermally fluctuating electric field gradients. Investigations of the spin-lattice relaxation of  $^{23}\text{Na}$ -NMR lines and of  $^{14}\text{N}$ -NQR lines above 77 K have been reported by Bonera et al. [1] and by G. Petersen et al. [2], respectively. They reported that the relaxation rate of the nuclear resonance lines simply decrease as the temperature decreases below room temperature.

However, in the lower temperature region, below 170 K, the temperature dependence of the spin-lattice relaxation time,  $T_1$ , of the  $^{14}\text{N}$ -NQR line in  $\text{NaNO}_2$  which has experienced some heating process, shows two minima around about 35 K and 70 K [3], and these minima are frequency dependent. On the other hand,  $T_1$  of a sample which was made by precipitation from an aqueous solution has no minimum in this temperature region and simply increases as the temperature decreases [4]. If the sample has been annealed below the melting temperature, the  $T_1$  minima ap-

peared on the curve of  $T_1 = f(T)$  [5]. It seems that this results can be ascribed to a relaxation center generated in course of the annealing treatment.

In the present study, the temperature dependence of  $T_1$  of the center line of  $^{23}\text{Na}$ -NMR in  $\text{NaNO}_2$  was observed for two different samples. They have been prepared by a modified Bridgman method and by a precipitation method from aqueous solution, respectively. Measurements were performed at three different external magnetic field strengths in order to study the frequency dependence of these properties.

## 2. Experimental

Two kinds of samples were used, a thermally heated one and non-heated one. Two single crystals measuring about  $0.8 \times 0.8 \times 1.5 \text{ cm}^3$  were prepared by a modified Bridgman method. We call them samples 1A and 1B. Measurements were performed mainly with the sample 1A. Crystal powder was made by precipitation from a saturated aqueous solution of  $\text{NaNO}_2$  as non-heated sample. We call it sample 2.

The spin-lattice relaxation time of the resonance line was measured by the  $\frac{\pi}{2} - \tau - \frac{\pi}{2}$  method using a pulse NMR spectrometer. The field  $B_0$  was 1.1, 4.7, and 6.9 Tesla in order to explore the frequency dependence of  $T_1 = f(T)$ . The external static magnetic field was chosen parallel to the crystal axis  $c$  in the measurements on the samples 1A and 1B. The error in the angles between  $B_0$  and the  $c$ -axis was within  $\pm 1^\circ$  for  $B_0 = 1.1$  Tesla, and  $\pm 5^\circ$  for  $B_0 = 4.7$  and 6.9 Tesla.

\* Presented at the XIth International Symposium on Nuclear Quadrupole Resonance Spectroscopy, London, United Kingdom, July 15–19, 1991.

<sup>1</sup> Present address: The meteorological agency, Hakodate, Hokkaido, Japan.

<sup>2</sup> Present address: The Furukawa electronic industry Co. Ltd., Chiba, Japan.

Reprint requests to Prof. Dr. Y. Abe, Institute of Physics, University of Tsukuba, Tsukuba, Ibaraki 305/Japan.

0932-0784 / 92 / 0100-0313 \$ 01.30/0. – Please order a reprint rather than making your own copy.



Dieses Werk wurde im Jahr 2013 vom Verlag Zeitschrift für Naturforschung in Zusammenarbeit mit der Max-Planck-Gesellschaft zur Förderung der Wissenschaften e.V. digitalisiert und unter folgender Lizenz veröffentlicht: Creative Commons Namensnennung-Keine Bearbeitung 3.0 Deutschland Lizenz.

Zum 01.01.2015 ist eine Anpassung der Lizenzbedingungen (Entfall der Creative Commons Lizenzbedingung „Keine Bearbeitung“) beabsichtigt, um eine Nachnutzung auch im Rahmen zukünftiger wissenschaftlicher Nutzungsformen zu ermöglichen.

This work has been digitalized and published in 2013 by Verlag Zeitschrift für Naturforschung in cooperation with the Max Planck Society for the Advancement of Science under a Creative Commons Attribution-NoDerivs 3.0 Germany License.

On 01.01.2015 it is planned to change the License Conditions (the removal of the Creative Commons License condition “no derivative works”). This is to allow reuse in the area of future scientific usage.

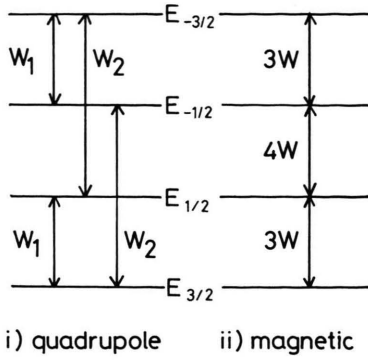


Fig. 1. Energy diagrams of  $^{23}\text{Na}$ -NMR and transition probability between them for the case of quadrupole and magnetic relaxation.

### 3. Method of Analysis

We will describe the recovery laws for the quadrupole and magnetic dipole-dipole relaxation process.

At first, we formulate them for the quadrupole relaxation [1]. We define the transition probability for  $\Delta m = \pm 1$  as  $W_1$  and that for  $\Delta m = \pm 2$  as  $W_2$ , as shown in Figure 1. Then, the rate equations are

$$\frac{dn_{-3/2}}{dt} = -(W_1 + W_2) \cdot n_{-3/2} + W_1 \cdot n_{-1/2} + W_2 \cdot n_{1/2}, \quad (1)$$

$$\frac{dn_{-1/2}}{dt} = W_1 \cdot n_{-3/2} - (W_1 + W_2) \cdot W n_{-1/2} + W_2 \cdot n_{3/2}, \quad (2)$$

$$\frac{dn_{1/2}}{dt} = W_2 \cdot n_{-3/2} - (W_1 + W_2) \cdot W n_{1/2} + W_1 \cdot n_{3/2}, \quad (3)$$

$$\frac{dn_{3/2}}{dt} = W_2 \cdot n_{-1/2} + W_1 \cdot n_{1/2} - (W_1 + W_2) \cdot n_{3/2} \quad (4)$$

where  $n_{-3/2}$ ,  $n_{-1/2}$ ,  $n_{1/2}$ , and  $n_{3/2}$  are population differences between the equilibrium value and the one at the time  $t$ , for each energy level. The eigenvalues of these equations are  $W_1$ ,  $W_2$ ,  $W_1 + W_2$ .

If we take as the initial condition that only the center line is saturated, a recovery function for the center line is calculated to be

$$\frac{S(\infty) - S(t)}{S(\infty)} = \frac{1}{2} (e^{-2W_1 t} + e^{-2W_2 t}). \quad (5)$$

For the case in which only one of the satellite lines is saturated, the recovery law of the irradiated satellite

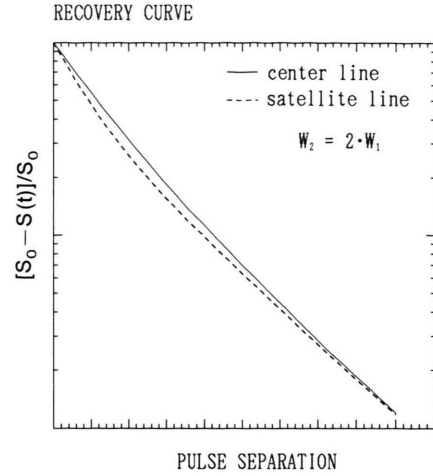


Fig. 2. Theoretical recovery curve of magnetization in case of a quadrupole relaxation and  $W_2 = 2 \cdot W_1$ .

lines is

$$\frac{S(\infty) - S(t)}{S(\infty)} = \frac{1}{2} (e^{-2W_1 t} + e^{-2(W_1 + W_2)t}). \quad (6)$$

We can see from (5) and (6) that the initial slopes of the recovery curve for the satellite lines are steeper than that for the center line, see Figure 2.

Then, we consider the recovery law in the case of the dominant magnetic dipole-dipole relaxation. The transition probability is zero except for the transition  $\Delta m = \pm 1$ , as shown in Fig. 1, where we define it as  $|<I|>|^2 \cdot W$ . That is, we use  $W$  for the value except the part concerning the operator. The rate equations in this case are [6],

$$\frac{dn_{-3/2}}{dt} = -3W \cdot n_{-3/2} + 3W \cdot n_{-1/2}, \quad (7)$$

$$\frac{dn_{-1/2}}{dt} = 3W \cdot n_{-3/2} - (4+3)W \cdot n_{-1/2} + 4W \cdot n_{1/2}, \quad (8)$$

$$\frac{dn_{1/2}}{dt} = 4W \cdot n_{-1/2} - (4+3)W \cdot n_{1/2} + 3W \cdot n_{3/2}, \quad (9)$$

$$\frac{dn_{3/2}}{dt} = 3W \cdot n_{1/2} - 3W \cdot n_{3/2}, \quad (10)$$

where  $n_{-3/2}$ ,  $n_{-1/2}$ ,  $n_{1/2}$ , and  $n_{3/2}$  are defined in the same way as in the quadrupolar case. The eigenvalues of these equations are  $2W$ ,  $6W$ , and  $12W$ . If only the center line is initially saturated, the recovery function

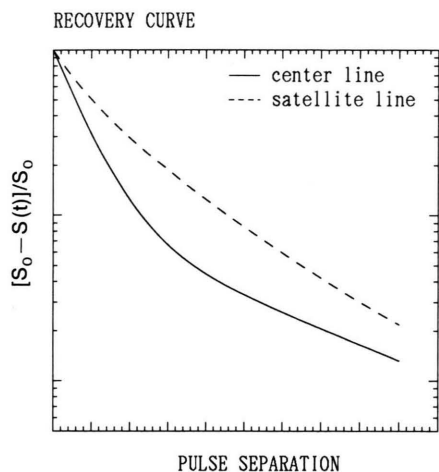


Fig. 3. Theoretical recovery curve of magnetization in case of magnetic relaxation.

will be [7]

$$\frac{S(\infty) - S(t)}{S(\infty)} = \frac{1}{10} e^{-2wt} + \frac{9}{10} e^{-12wt}. \quad (11)$$

For the condition that only one of the satellite lines is initially saturated, the successive recovery of the same satellite line is calculated to be

$$\frac{S(\infty) - S(t)}{S(\infty)} = \frac{1}{10} e^{-2wt} + \frac{5}{10} e^{-6wt} + \frac{4}{10} e^{-12wt}. \quad (12)$$

These equations indicate that the recoveries of the satellite lines are slower than that of the center line, as shown in Figure 3.

Thus, by comparing the recovery curves of the satellite lines and of the center line we can distinguish whether the relaxation process is quadrupolar or magnetic.

#### 4. Results and Discussion

The temperature dependences of  $T_1$  of the center line of  $^{23}\text{Na}$ -NMR in the two samples 1B and 2 at 53.4 MHz ( $B_0 = 4.7$  Tesla) are shown in Figure 4. The values of  $T_1$  are determined by fitting a single exponential recovery function to the initial slopes of the experimental data. We see that  $T_1^{-1}$  of sample 1B has two maxima around 44 K and 95 K, but for the precipitated sample it simply decreases as the temperature decreases. (There are no data below 77 K, but in

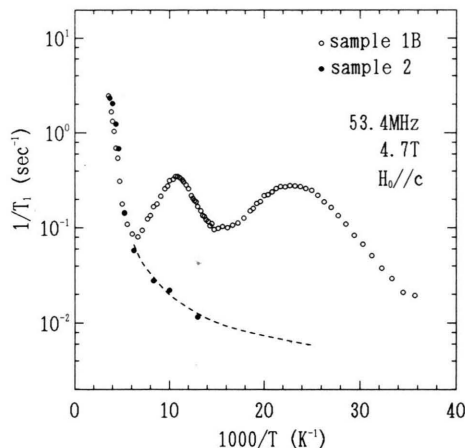


Fig. 4. The temperature dependence of the spin-lattice relaxation rate  $T_1$  of the center line of  $^{23}\text{Na}$ -NMR in  $\text{NaNO}_2$  at 53.4 MHz (4.7 T). The dashed line is an eye guide for sample 2.

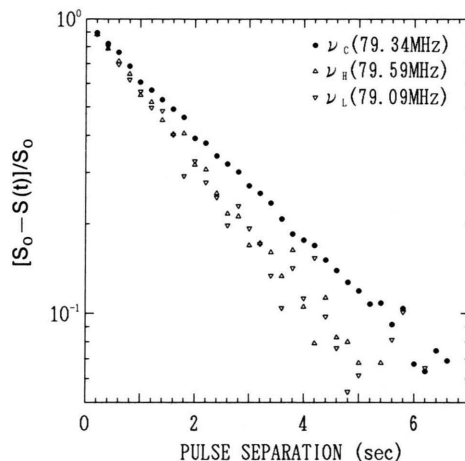


Fig. 5. Magnetization recovery at 220 K,  $B_0 = 6.9$  T.  $\nu_c$  stands for center line,  $\nu_H$  represents the satellite line whose resonance frequency is higher than that of the center line and  $\nu_L$  represents lower one. This definition is valid in Figs. 5–8.

the case of  $^{14}\text{N}$ -NQR,  $T_1^{-1}$  simply decreases as the temperature decreases. Thus it seems that the intrinsic relaxation is small in the low temperature region. Therefore we look on it as a simple decreasing curve.) This result is expected from the experiments on the  $^{14}\text{N}$ -NQR line.

Figures 5, 6, 7, and 8 show the precise recovery curve of the center line and the satellite lines in the sample 1A at 220, 115, 94, and 44 K at 79.3 MHz ( $B_0 = 6.9$  Tesla). The chosen temperatures 94 K and 44 K are located at the two minima.  $T_1$  at 220 K

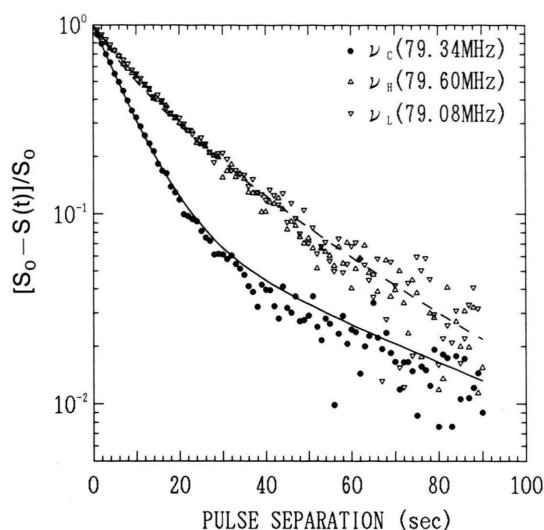


Fig. 6. Magnetization recovery at 115 K,  $B_0 = 6.9$  T. The solid line is calculated with (11). The dashed line is calculated with (12) and the fitting parameters of the center line. The lines in Figs. 7 and 8 are drawn in a similar way.

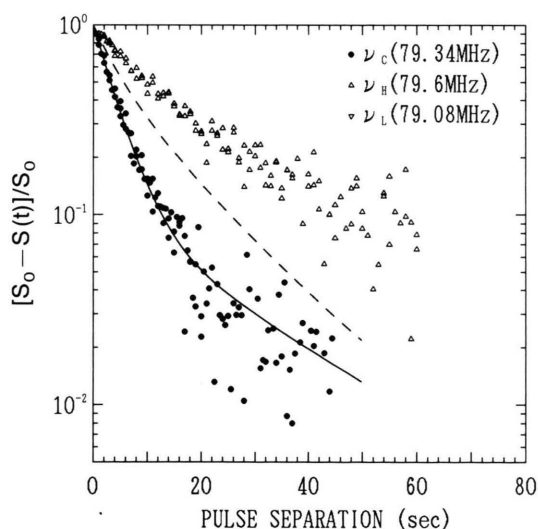


Fig. 7. Magnetization recovery at 94 K,  $B_0 = 6.9$  T.

slightly depends on the way to prepare a sample. The satellite lines recover more rapidly than the center line at 220 K. But in contrast with this, the center lines relax more rapidly than the satellite lines at the other temperatures. This phenomenon suggests that the dominant relaxation mechanism in the low temperature region ( $\leq 150$  K) is different from the one in the high temperature region ( $\geq 170$  K).

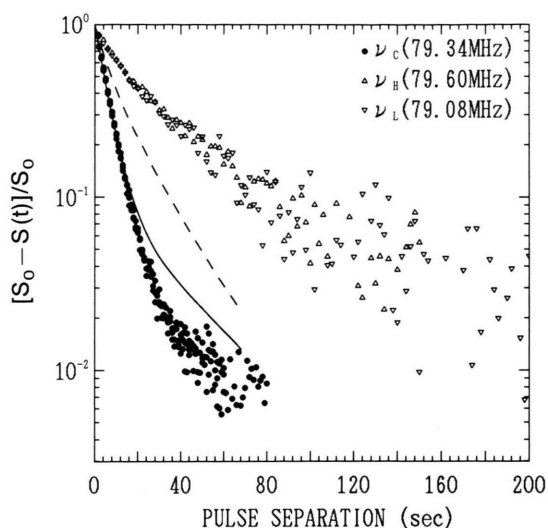


Fig. 8. Magnetization recovery at 44 K,  $B_0 = 6.9$  T.

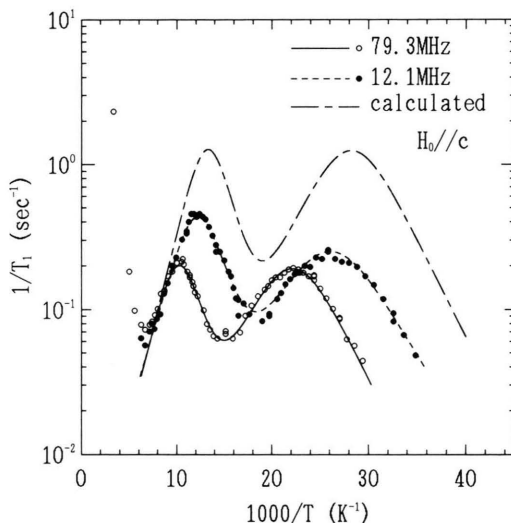


Fig. 9. Temperature dependence of  $T_1$  of the center line of  $^{23}\text{Na}$ -NMR in  $\text{NaNO}_2$  at 1.1 T (12.1 MHz) and 6.9 T (79.3 MHz) for sample 1A. The solid and dashed lines are calculated by application of (13) to each data point. The dash-dotted line is drawn by calculating (13) for 12.1 MHz, using the fitting parameter at 79.3 MHz.

The solid lines in Figs. 6, 7, and 8 are the best fit of (11) to the recovery curve of the center line. Using the factor  $W$  which is determined by this fitting, the dashed lines in the figures are calculated from (12). At 115 K and 94 K, the solid lines almost approximate the recovery curves. But the solid line is not well fitted by (12) at 44 K. We can not yet show the reason of this phenomenon. One should think about a rather differ-

ent mechanism for these phenomena. But, from a qualitative point of view, it seems that the relaxation mechanism in the low temperature region is magnetic rather than quadrupolar because the initial slope of the recovery curve of the magnetization for the center line is steeper than that for satellite lines.

Figure 9 shows the temperature dependence of  $T_1$  of the center line of the  $^{23}\text{Na}$ -NMR in  $\text{NaNO}_2$  at 12.1 and 79.3 MHz. We can make sure that their behaviour depends on the resonance frequency.

In order to explain this frequency dependence, we suppose that the dominant relaxation mechanisms in this temperature region are of the BPP type [8] because there are two dips in the temperature dependence of  $T_1$ . We assume that the whole transition probability,  $W(\propto 1/T_1)$ , consists of two terms, and each term is described by a correlation time  $\tau$ . If  $\tau$  satisfies the Arrhenius's relation,  $W$  can be expressed as

$$W(T) = C_H \frac{\tau_H}{1 + (\omega\tau_H)^2} + C_L \frac{\tau_L}{1 + (\omega\tau_L)^2}, \quad (13)$$

$$\tau_H = \tau_{0H} \exp\left(\frac{E_{aH}}{kT}\right), \quad (14)$$

$$\tau_L = \tau_{0L} \exp\left(\frac{E_{aL}}{kT}\right), \quad (15)$$

where  $\omega = 2\pi\nu$ ,  $E_{aH}$  and  $E_{aL}$  are the activation energies,  $\tau_H$  and  $\tau_L$  are the correlation times, and  $C_H$  and  $C_L$  are constant coefficients which do not depend on the temperature and the resonance frequency. The subscripts  $H$  and  $L$  indicate whether the values  $E_a$ ,  $\tau$ ,  $\tau_0$ , and  $C$  belong to the one or the other of the two terms of the function. If the temperature dependence of  $T_1$  can be fitted by these equations with common  $E_a$ ,  $\tau_0$ , and  $C$ , we think that the relaxation processes are of the normal BPP type.

The solid line in the Fig. 9 is a fitted line of (13) to the data for the resonance frequency 79.3 MHz, and the dashed line is for 12.1 MHz. One can see that they fulfill (13), but the fitting parameters are rather different. The fitting parameters are shown in the Table 1. The dash-dotted line in the figure is calculated for 12.1 MHz, using the fitting parameters derived for the case at 79.3 MHz. As we see from the discrepancy between the dashed line and the dash-dotted line, the temperature dependence of  $T_1$  of the  $^{23}\text{Na}$ -NMR line can not be explained only by (13).

In order to show the discrepancy between the experimental data at 12.1 MHz and the calculated curve

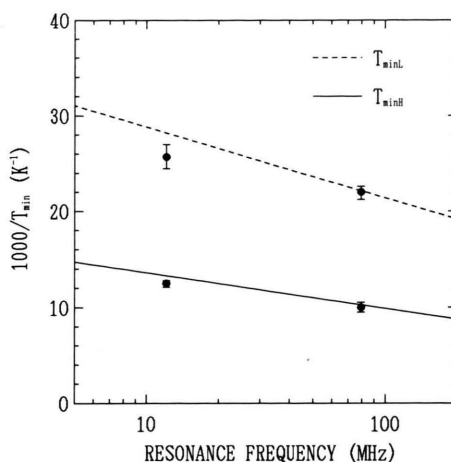


Fig. 10. Frequency dependence of  $T_{\min}^{-1}$ .  $T_{\min}$  is the temperature where  $T_1^{-1}$  takes a maximum value.

Table 1. Fitting parameters of (13) to the experimental data of the  $T_1 = f(T)$  curve.

Frequency	$E_{aH}$	$\tau_{0H}$	$E_{aL}$	$\tau_{0L}$
79.3 MHz	620 K	$3.5 \times 10^{-12}$ sec	310 K	$2.1 \times 10^{-12}$ sec
12.1 MHz	540 K	$1.8 \times 10^{-11}$ sec	260 K	$1.5 \times 10^{-11}$ sec

by using the parameters derived from the data at 79.3 MHz, we give a relation between the resonance frequency and the temperature where a minimum of  $T_1$  exists (we define the temperature as  $T_{\min}$ ). If the  $T_1$  minimum is given at a temperature where  $\omega \cdot \tau = 1$ ,  $\omega = 2\pi\nu$ , the relation between  $T_{\min}$  and  $\omega$  is given by solving (14) and (15) at  $T_{\min}$ :

$$\frac{1}{T_{\min}} = -\frac{k}{E_a} \cdot \{\ln(\omega) - \ln(\tau_0)\}. \quad (16)$$

This equation shows that  $T_{\min}^{-1}$  is linear to  $\ln(\omega)$ . Figure 10 shows experimental data of  $T_{\min}^{-1}$  and a plot of (16) using the parameters derived from the data at 79.3 MHz. The discrepancies between the experimental data and the plot of (16) is somewhat larger than the experimental error at 12.1 MHz.

There is another anomaly in the curve of the temperature dependence of  $T_1$ . If (13) is appropriate to this relaxation mechanisms, absolute values of  $T_1$  for lower resonance frequencies must be larger than that for higher frequencies at the same temperature except in the high temperature region above the dip which is located at the higher temperature side, as shown in Figure 11. But the experimental data clearly show that



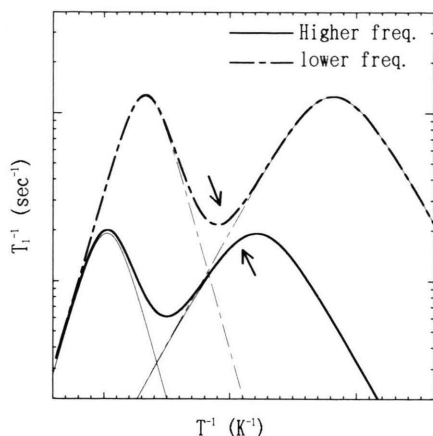


Fig. 11. Theoretical temperature dependence of the spin-lattice relaxation rate,  $T_1^{-1}$ , in two different magnetic fields, where we assume a BPP type relaxation mechanism. We use (13) to calculate each curve. They do not meet below the temperature where on the higher temperature side a maximum exists. But for the experimental data in Fig. 9, they intersect with each other between the higher side maximum and the lower side maximum, where arrows in the figure point at. This phenomenon shows that the relaxation mechanism which gives the two maxima of  $T_1^{-1}$  can not be fully explained by the simple BPP type model.

the absolute values of  $T_1$  for the lower resonance frequency (12.1 MHz) is smaller than that for the higher frequency (79.3 MHz) between about 45 K and 55 K. This fact suggests that the relaxation mechanism which gives the lower side dip is different from a BPP type relaxation mechanism.

## 5. Conclusion

The temperature dependence of  $T_1$  of the  $^{23}\text{Na}$ -NMR line in  $\text{NaNO}_2$ , which was prepared by a heating process, has two dips in the low temperature region. Their property depends on the resonance frequency. On the other hand, the non-heated sample, prepared by precipitation from aqueous solution, shows no minimum.

Comparing the recovery curve of the center line with those of the satellite lines, the dominant relaxation mechanism around the two dips is founded to be magnetic rather than quadrupolar. The temperature dependence of  $T_1$  can not be explained fully by a BPP type relaxation mechanism.

## Acknowledgement

This study was mainly performed at The Cryogenics Center of The University of Tsukuba.

- [1] G. Bonera, F. Borsa, and A. Rigamonti, *Phys. Rev. B* **2**, 2784 (1970).
- [2] G. Petersen and P. J. Bray, *J. Chem. Phys.* **64**, 522 (1976).
- [3] Y. Abe, Y. Ohneda, S. Abe, and S. Kojima, *J. Phys. Soc. Japan* **33**, 864 (1972).
- [4] Y. Abe, Y. Ohneda, and S. Kojima, unpublished paper.
- [5] M. Igarashi, K. Eto, Y. Saito, and Y. Abe, *Z. Naturforsch.* **45a**, 523 (1990).
- [6] E. R. Andrew and D. P. Tunstall, *Proc. Phys. Soc.* **78**, 1 (1961).
- [7] S. Towta and D. G. Hughes, *J. Phys. Condens. Matter* **2**, 2021 (1990).
- [8] N. Bloembergen, E. M. Purcell, and R. V. Pound, *Phys. Rev. B* **73**, 679 (1948).